

TURN ON MECHANISM OF 2500V MOS ASSISTED GATE TRIGGERED THYRISTER (MAGT)

Akio Nakagawa, Hirotohi Yoshida and Yoshio Kamei

Toshiba Corporation Research & Development Center
1 Komukai Toshibacho, Saiwai-ku, Kawasaki, 210, Japan

ABSTRACT

2500V MOS Assisted Gate Triggered Thyristors (MAGTs) have been proposed as promising devices for future pulsed power applications. It was successfully demonstrated that the device is able to form an extremely large current pulse of $110\text{kA}/\mu\text{sec}/\text{cm}^2$ di/dt and 100nsec pulse width.

Numerical simulations were carried out to investigate the switching-on mechanism as well as the maximum switching speed. It was found that three operation modes are distinguishable in the turn-on transients and that the whole device area goes into thyristor action only 45nsec after MOS gate triggering. These results support the possibility that MAGTs directly replace thyristors in the near future.

INTRODUCTION

Extremely large current-pulse formation in a short time period is a promising future technology for pulsed power applications such as power supplies for excimer lasers, particle accelerators etc.

Currently, thyristors are widely used for such applications, although their lifetime is limited. A variety of efforts have been made to replace conventional thyristors by using currently available semiconductor devices[1]. MOS Assisted Gate Triggered Thyristors, MAGTs[2], have been proposed as semiconductor devices for such key switching applications, having the potential to replace conventional thyristors. It has been reported[3] that the 2500V MAGTs achieved fast di/dt turn-on, exceeding $40\text{kA}/\mu\text{s}/\text{cm}^2$.

Figure 1 shows a schematic cross section of a MAGT with two control gates. One is an ordinary MOS gate. The other is a current control gate, called a "base electrode", which is electrically connected to the P-base layer. A MAGT is basically triggered by the MOS gate. The base electrode is used to prevent a MAGT from miss-triggering. A $1000\text{V}/\mu\text{sec}$ dV/dt immunity can be achieved by negatively biasing the base electrode in the off-state.

MAGTs are distinguished from conventional MOS thyristors[4] or IGBTs in the sense that no emitter-shorts exist throughout the device and, thus, the cathode and the base electrodes are completely separated. This makes it possible to realize fine patterned MAGTs while keeping high NPN transistor current gains for rapid triggering.

In this paper, we investigate the triggering mechanism of MAGTs and predict the possibility for

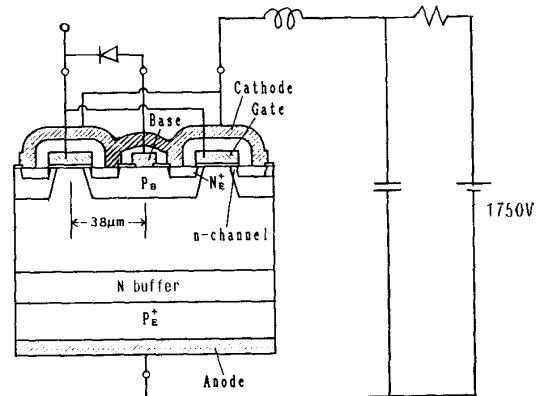


Fig.1 Calculated MAGT structure, gate terminal arrangement and external circuits

rapid triggering using a device simulator TONADDEIC[5].

SIMULATION OF MAGT TURN-ON

The authors carried out rigorous numerical simulations of the MAGT turn-on process using the device simulator TONADDEIC. A calculated device was turned-on from a 1750V off-state with $2.1\text{kA}/\mu\text{sec}/\text{cm}^2$ anode current rise rate (di/dt). External circuit parameters (inductor and capacitor values) were chosen in such a way that the oscillating pulse width was $2.5\mu\text{sec}$ and peak current density $1800\text{A}/\text{cm}^2$.

Figure 1 shows the calculated MAGT structure. The half device size for the calculated device region is $38\mu\text{m}$. An N-buffer layer has been introduced, for the first time, in this particular device structure to enhance the switching speed. The adopted circuit configuration is also shown in the figure.

Figure 2 shows the calculated turn-on waveform. The gate voltage was raised from -2.5V to 12.5V in 10nsec . The calculated turn-on time was as extremely short as 9nsec and the rise time was only 4nsec . The anode voltage (forward voltage) decreased from 1750V to below 100V within 100nsec . Figure 3 shows the experimentally obtained turn-on waveform under similar conditions for comparison. Simulated waveforms precisely agree with the experimental results.

Since an N-buffer layer is adopted, the whole N-base region was depleted upon application of 1750V . Figures 4 and 5 show 3-dimensional electron and hole

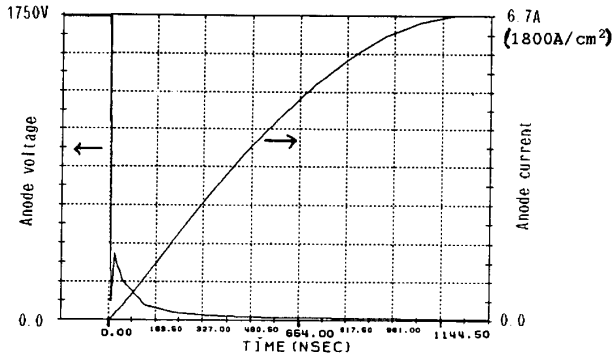


Fig. 2 Calculated turn-on characteristics.

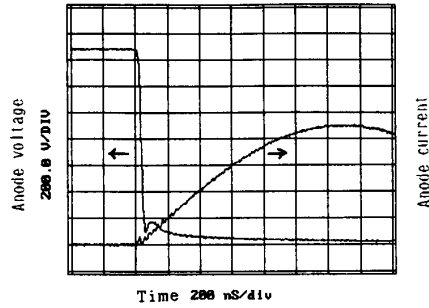


Fig. 3 Experimentally obtained turn-on characteristics under similar conditions to Fig. 2.

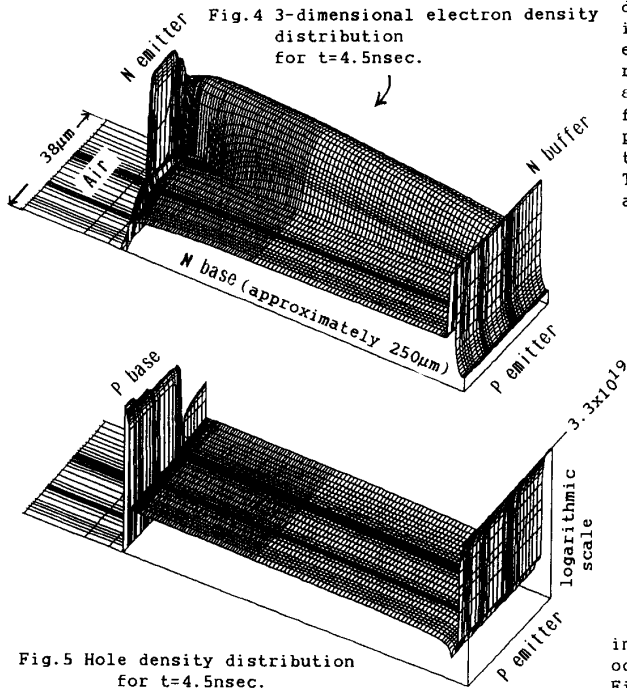


Fig. 5 Hole density distribution for t=4.5nsec.

density plots for the 4.5nsec time step. It is clear that electron injection into the N-base occurs immediately after creation of the channel, although the applied gate voltage for the 4.5nsec time step is 4.3V, which is only slightly above the threshold voltage (approximately 3V). This rapidly decreases the device forward voltage in the early stages of turn-on because the total device current is small due to the nature of the inductive load. The device on-resistance itself, however, is still quite high because only electrons conduct current and conductivity modulation does not yet occur. It should be noted that the anode voltage had already decreased to 110V when the gate voltage reached 12.5V in the 10nsec time step.

Figure 6 shows the net electron particle current distribution along the Y-axis. It is quite interesting that the electron current greatly exceeds the total anode current of $9.05 \times 10^{-5} \text{A}$. The reason for this is simple. The displacement current $\epsilon \partial E / \partial t$, caused by the decrease in anode voltage, flows in the opposite direction to the electron particle current. Thus, the total current remains the same as the anode current through the device. This enhances electron injection into the N-base, and accelerates the anode voltage decrease.

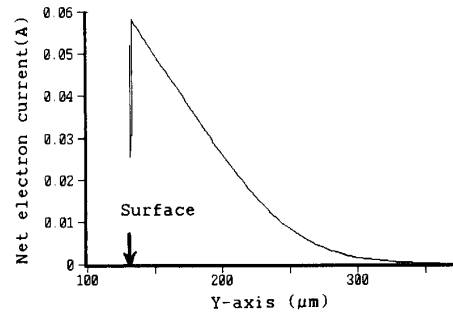


Fig. 6 Net electron particle current distribution along Y-axis.

It is also an interesting fact that hole injection from the anode emitter had not yet occurred in the 4.5nsec time step, as is shown in Figs. 4 and 5. Figure 7 shows electron and hole particle current distributions across the N-buffer P-emitter junction, corresponding to Figs. 4 and 5. Hole injection into the N-base had not occurred at this stage, accompanying the 5nsec time delay from the electron injection. (Naturally, the current across the junction is carried wholly by the displacement current.) This delay time is necessary to forward bias the N-buffer P-emitter junction and to charge up the junction capacitance.

The device forward voltage decreased to 110V at the 10nsec time step mostly due to electron injection into the N-base. However, the voltage rapidly increased again to 311V as the drain current increased. Although hole injection had started to occur and the device began to operate in a similar mode to that of an IGBT (see Figs. 8 and 9), this was not sufficient to decrease the forward voltage but

32.7.2

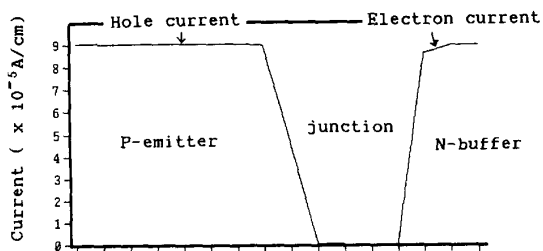


Fig. 7 Electron and hole particle current across N-buffer P-emitter junction.

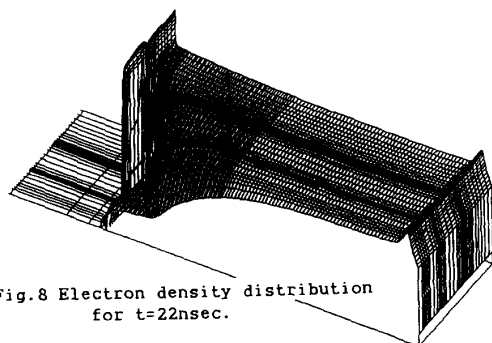


Fig. 8 Electron density distribution for t=22nsec.

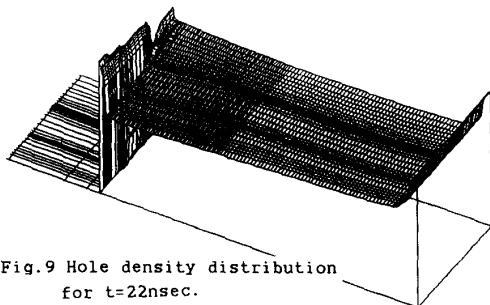


Fig. 9 Hole density distribution for t=22nsec.

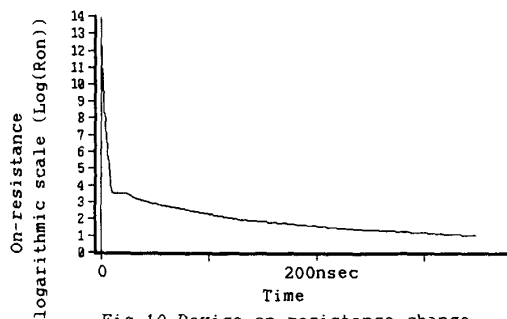


Fig. 10 Device on-resistance change with time step

only to maintain the device on-resistance at the same level, while the anode current kept increasing. The change in device on-resistance with time, as shown in Fig. 10, clearly reflects these phenomena. The on-resistance first rapidly decreases because of electron injection into the N-base while the gate voltage rises from -2.5V to 12.5V in 10nsec. From 10nsec to 22nsec, the device resistance remains constant although the device starts to operate in the IGBT mode. The device resistance again gradually decreases after the device begins thyristor action (latch up).

It is seen in Figs. 11 and 12 that 45nsec is sufficient for the MAGT to reach complete thyristor action over the whole device area. This implies that MAGTs can be operated with a 100nsec pulse width, and this was actually confirmed experimentally and will be described in the next section.

The calculated results also imply that if the device cell size is small, it is quite possible to uniformly trigger the whole device area with the MOS gate.

EXPERIMENTAL

2500V MAGTs were fabricated to confirm the switching-on characteristics predicted by the numerical simulation. N-buffer layers were adopted to enhance switching speed. Two aluminum layers with polyimide insulation layers for cathode and P-base electrodes were introduced to reduce the unit-cell size.

Since the N-base layer is as thin as 250um, the silicon wafer direct-bonding technique [6] was adopted to realize a high resistivity N-base layer on an N-buffer layer. Details of the wafer fabrication process were the same as for 1800V IGBTs (see ref. [7]). Figure 13 shows a fabricated chip overview (3.3mm by 4.9mm chip).

It was confirmed that MAGTs can be operated with 100nsec pulse widths, as seen in Fig. 14. The observed di/dt exceeded $100\text{kA}/\mu\text{sec}/\text{cm}^2$, which is, to the authors' knowledge, the largest value ever reported in semiconductor devices. MAGTs also have a large current handling capability, exceeding $10\text{kA}/\text{cm}^2$ for a 7V forward voltage. Thus, they have a great potential to directly replace conventional thyristors.

It is also noticeable in Fig. 14 that the rise time is as long as 50nsec and that most power dissipation occurs within this period. Figure 15 shows the dependence of turn-on power loss on pulse width, if 5kpps operation is assumed. Power loss in the rise time period represents a considerable portion of total power loss when the pulse width is less than 300nsec. A 0.6 or 0.7μsec pulse width operation is most suitable for these MAGTs.

The phenomena occurring inside the device are assumed to be basically the same as those calculated in the low di/dt case. The difference is that the anode voltage does not rapidly decrease until the device reaches thyristor action.

DISCUSSION

MAGTs can be switched on also by the base electrode. If the base current is sufficient, the same switching speed can be attained by base triggering. The authors assume that MOS gate triggering is superior to base triggering because

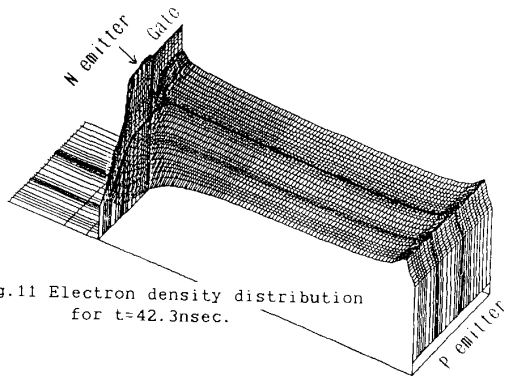


Fig.11 Electron density distribution for $t=42.3\text{nsec}$.

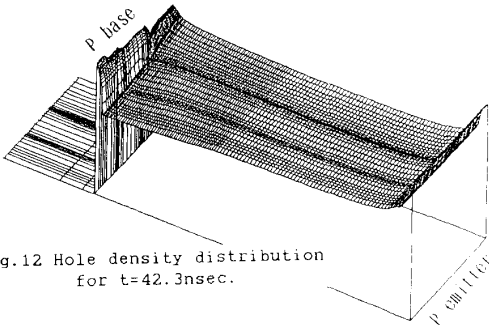


Fig.12 Hole density distribution for $t=42.3\text{nsec}$.

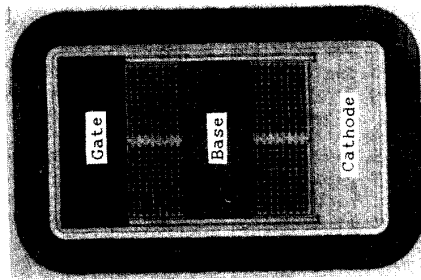


Fig.13 Fabricated device overview. (3.3mm x 4.9mm)

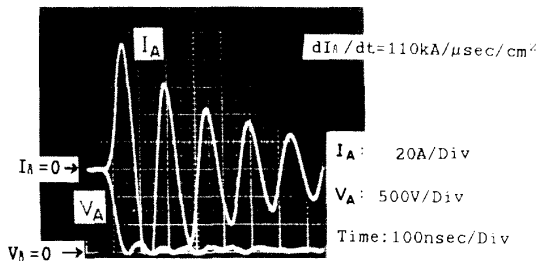


Fig.14 100nsec pulse operation of fabricated MAGT.

uniform triggering over a large chip area is more easily attained using a MOS gate. Moreover, the MOS and the base electrodes can be connected through a diode, so that the MAGT can be treated as if it were a three terminal device. The detailed arrangement is described in Fig.1.

CONCLUSION

This paper clearly demonstrates the basic triggering mechanism and the high di/dt capability, a result of the fact that the whole device area reaches thyristor action only 45nsec after gate triggering. This is attributed to the fine-patterned small unit cell size and uniform MOS gate triggering. MAGTs also have a large current handling capability, exceeding $10\text{kA}/\text{cm}^2$, and thus have great potential as a direct replacement for conventional thyristors.

*A part of this work was accomplished under the Research and Development on "Advanced Material Processing and Machining System", conducted under a program set up by the New energy and Industrial Technology Development Organization.

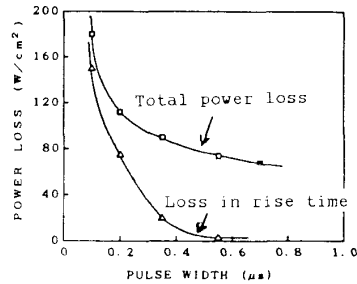


Fig.15 Switching-on power loss dependence on oscillating current pulse width.

REFERENCES

- [1] W.M.Portnoy, Proceeding of ISPSD'90, p.2
- [2] T. Shinohe, et al, 1989 IEEE IEDM Technical Digest, p.301
- [3] T. Shinohe, et al, Proceeding of ISPSD'90, p.277.
- [4] J.Tihany, 1980 IEEE IEDM Tech. Dig. p.75
- [5] A.Nakagawa et al, Proceeding of NASECODE-V, p.295.
- [6] M.Shimbo et al, J.Appl.Phys., vol.48, p.78(1986)
- [7] A.Nakagawa et al, 1986 IEEE IEDM Tech. Dig., p.122.